14.4 THE MODULATION OF CANYON FLOWS BY LARGER-SCALE INFLUENCES

Lisa S. Darby and Robert M. Banta
NOAA/Earth System Research Laboratory, Boulder, CO 80305

1. INTRODUCTION

During October of 2000, the Vertical Transport and Mixing (VTMX) campaign, sponsored by the United States Department of Energy, took place in the Salt Lake City basin (Doran et al. 2002). The geography of the basin presented the opportunity to study a variety of meteorological phenomena associated with complex terrain. The basin is bounded by mountain ranges to the west, south, and east (Fig. 1). The Traverse Mountains to the south are lower in elevation than the Oquirrhs and Wasatch, and have a gap, the Jordan Narrows, that allows the penetration of a southerly low-level jet (LLJ) into the basin at night (Banta et al. 2004). The Wasatch Range has several major canyons that drain into the basin. Because of these terrain features, and the Great Salt Lake to the northwest of the basin, there are many types of predictable flows associated with the diurnal cycle (e.g., lake breeze, slope flows, and drainage flows). Although the dynamics behind these flows may be well understood, the details of the structure of these flows, as well as their impact on cold pool formation and destruction, air quality in the basin, and transport and diffusion, for example, were not well understood.

The National Oceanic and Atmospheric Administration/Earth System Research Laboratory (NOAA/ESRL) deployed a scanning Doppler lidar to the basin for the VTMX campaign (Banta et al. 2004, Fast and Darby 2004, Darby et al. 2006). Doppler lidar is ideally suited to obtain wind measurements in complex terrain because of its narrow beam and lack of ground clutter. We measured winds above the mountain barriers, winds within the basin, and embedded smaller-scale flow features. By combining measurements focused on these flows, which occur on different spatial and temporal scales, we can assess the interplay among the flow features.

In this study, we are interested in isolating the effects of larger-scale flows on the penetration of nighttime canyon outflows into the Salt Lake City basin. Before VTMX, the extent of the penetration of the canyon outflows into the basin was not fully appreciated, because the outflows are usually elevated as they extend into the basin, and therefore are not measured by ground-based anemometers, except near the canyon mouths. Canyon outflows are important for several reasons. Outflows introduce air into the basin that is “cleaner”, i.e., has lower aerosol content, and colder. The outflows can create vertical mixing through convergence with basin-scale flows and through directional shear with height. At the surface, the outflows create small-scale eddies, or flow reversals, near the mouths of the canyons. These eddies play a role in the inhibition of pollutant transport, particularly near the downtown Salt Lake City region (Darby et al. 2006).

To assess the large-scale flows, we look at the wind speed and direction above the ridge-tops of the bounding mountains and the southerly LLJ. To assess the penetration of canyon outflows, we look at lidar scans pointing toward the openings of the major canyons. We focus on the timing, depth, speed, and maximum height of the canyon outflows and the LLJ.

2. BACKGROUND INFORMATION

During VTMX the NOAA/ESRL Doppler lidar employed 2 basic scanning patterns to measure radial velocity: 1) scanning in azimuth while maintaining a constant elevation angle (referred to as conical scans, Fig. 2), and 2) scanning in elevation while maintaining a constant azimuth angle (referred to as range-height (R-H) scans, Fig. 3). From conical scans we derived vertical profiles of the horizontal wind, using the method of Browning and Wexler (1968). The wind profiles extended above the ridge-tops of the bounding mountain ranges (Wasatch and Oquirrhs, Fig. 1).

R-H scans were taken toward the openings of all major canyons that drain into the Salt Lake City basin. The radial velocity measurements from the canyon R-H scans (in spherical coordinates) were converted to the wind component parallel to the plane of the R-H scan (on a Cartesian grid), a standard method

---

Corresponding author address: Lisa S. Darby, NOAA/ESRL, CSD3, 325 Broadway, Boulder, CO, 80305; email: Lisa.Darby@noaa.gov

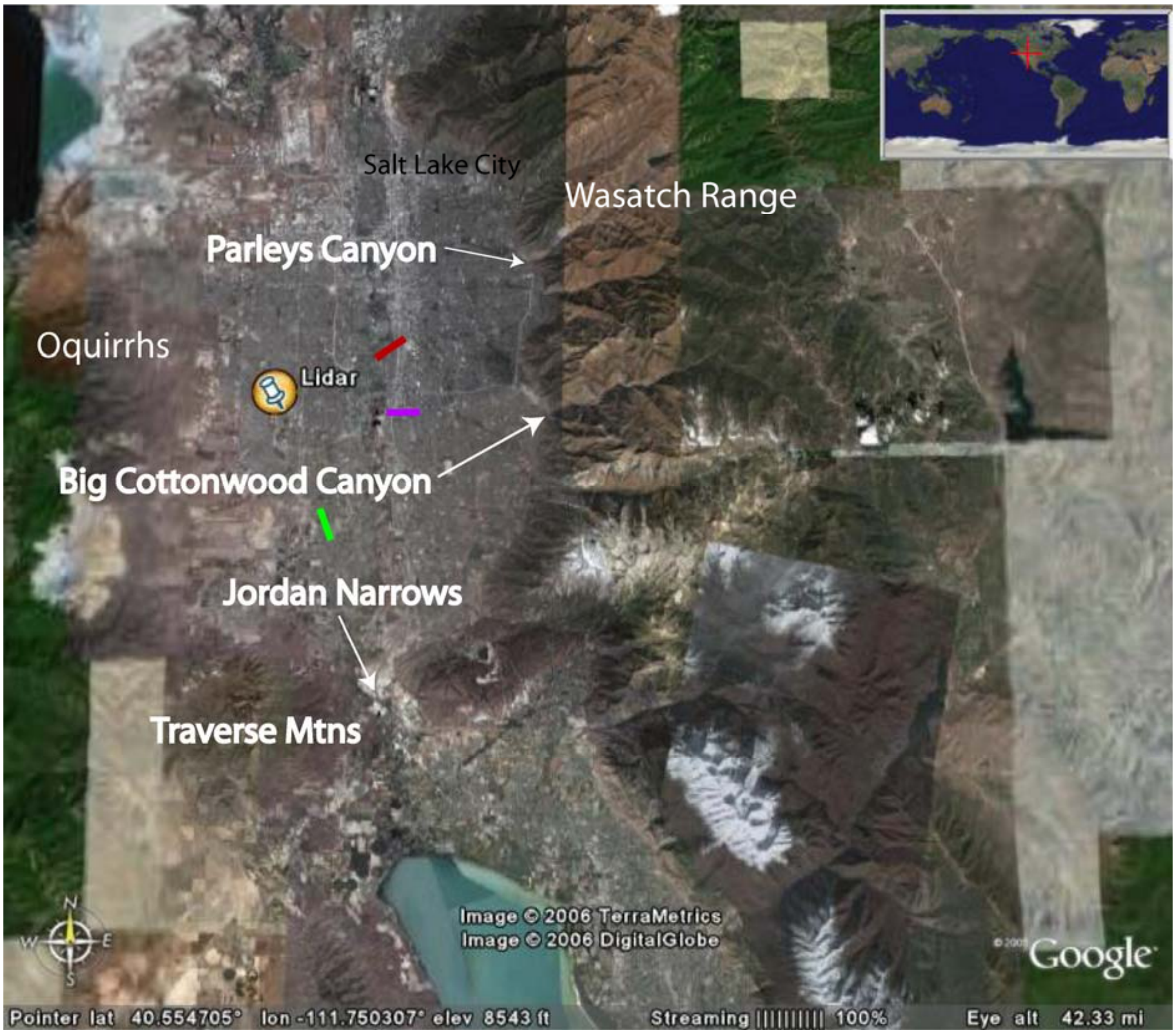

Figure 1: Google Earth satellite composite of the Salt Lake City basin and surrounding terrain. The location of the NOAA/ESRL Doppler lidar is indicated with the push-pin symbol. Important terrain features are labeled. The colored boxes indicate the approximate locations of the lidar data used to construct the time-height series of the wind component parallel to the plane of the range-height scans pointing toward: 1) Parleys Canyon (red box), 2) Big Cottonwood Canyon (magenta box), and 3) Jordan Narrows (green box).

for analyzing Doppler lidar R-H wind measurements (see Banta et al. 1993 for more detail on the method). To create profiles of the horizontal wind, we averaged the horizontal wind at each gridded height from a window 7 to 9 km horizontal range from the lidar (Fig. 1), and then combined the profiles into a time-height series for each IOP (Figs. 5-9). This 7-9 km window was chosen because it was the window farthest away from the lidar with consistently adequate signal strength to perform the calculations for all IOPs of interest. For brevity, we will only present measurements for Parleys (PAR) and Big Cottonwood (BCC) Canyons (Fig. 1).

During the Intensive Operating Periods (IOPs) chosen for discussion, the synoptic scale setting was such that local-scale, thermally-driven flows were allowed to form. [For an overview of the meteorology and character of the IOPs, see Doran et al. (2002) and Fast and Darby (2004).] In the course of our analysis it became apparent that the southerly LLJ that occurred during all IOPs presented here had an impact on the penetration of the canyon outflows into the basin,

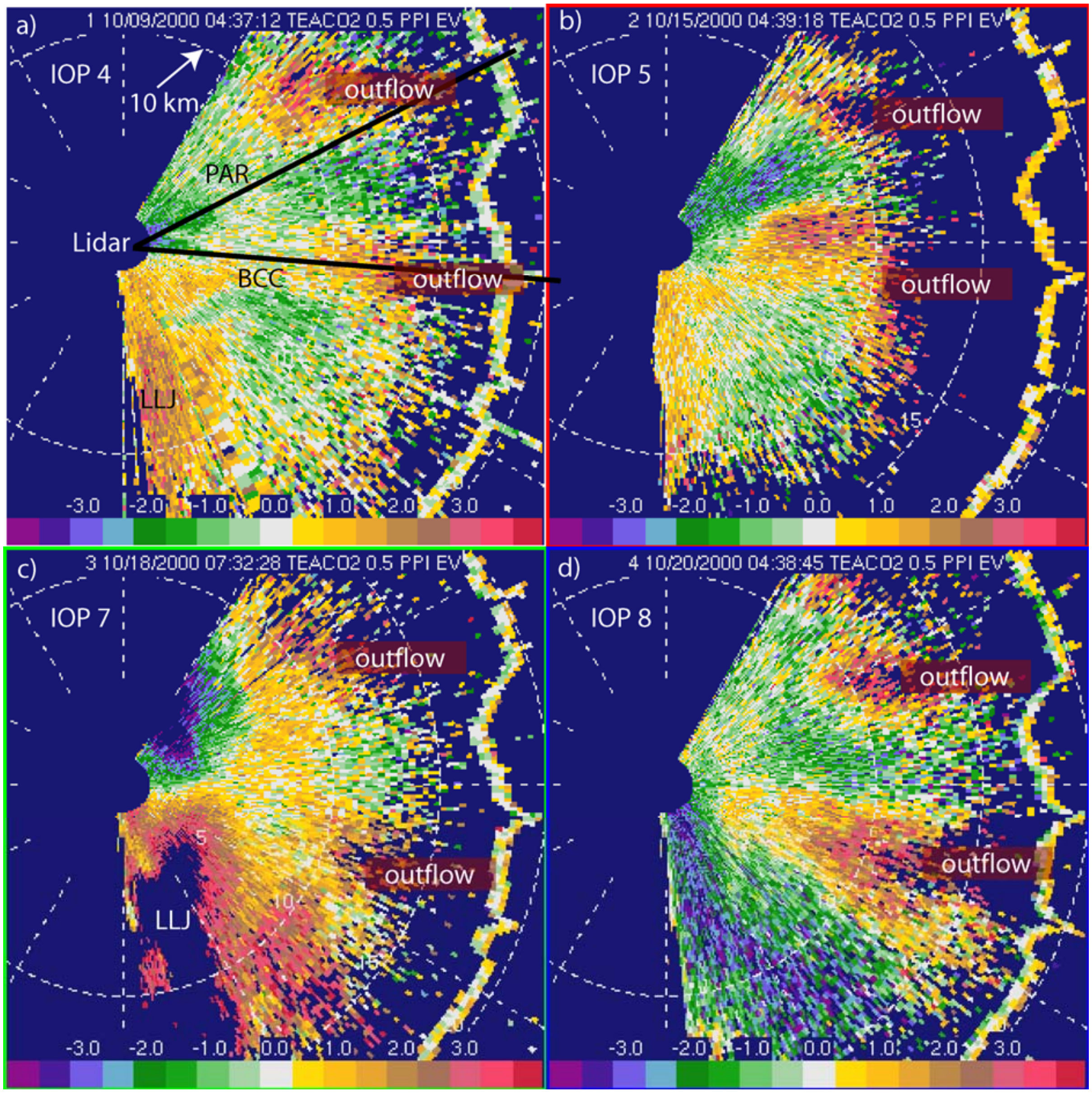

Figure 2: Nearly-horizontal (elevation angle = 0.5°) Doppler lidar radial velocity scans for a) IOP 4, b) IOP 5, c) IOP 7, and d) IOP 8. The color bar at the bottom of each scan represents radial velocity in m s^{-1} and is set to enhance the canyon outflows, which are labeled. Positive velocity indicates flow toward the lidar. The solid returns to the east (right) of the lidar are terrain hits. The black lines in a) point toward Parleys Canyon and Big Cottonwood Canyon, the two canyons featured in the paper. In c) the low-level jet from the south was strong enough that the radial velocities were off-scale. Times are UTC (Local standard time = UTC -7 hours).

therefore we organize our discussion around the establishment of the LLJ.

In our discussion, “outflow” refers to wind flow with a component out of the canyon toward the basin center, represented by negative (dashed) contours in the time-height series. The presence of an outflow can be confirmed by looking at the low-elevation angle conical scans, as in Fig. 2. “Inflow” refers to flow with a component from the basin toward the canyon and is represented by positive (solid) contours in the time series. We seek to relate these inflows and outflows to both the basin-scale and ridge-top winds.

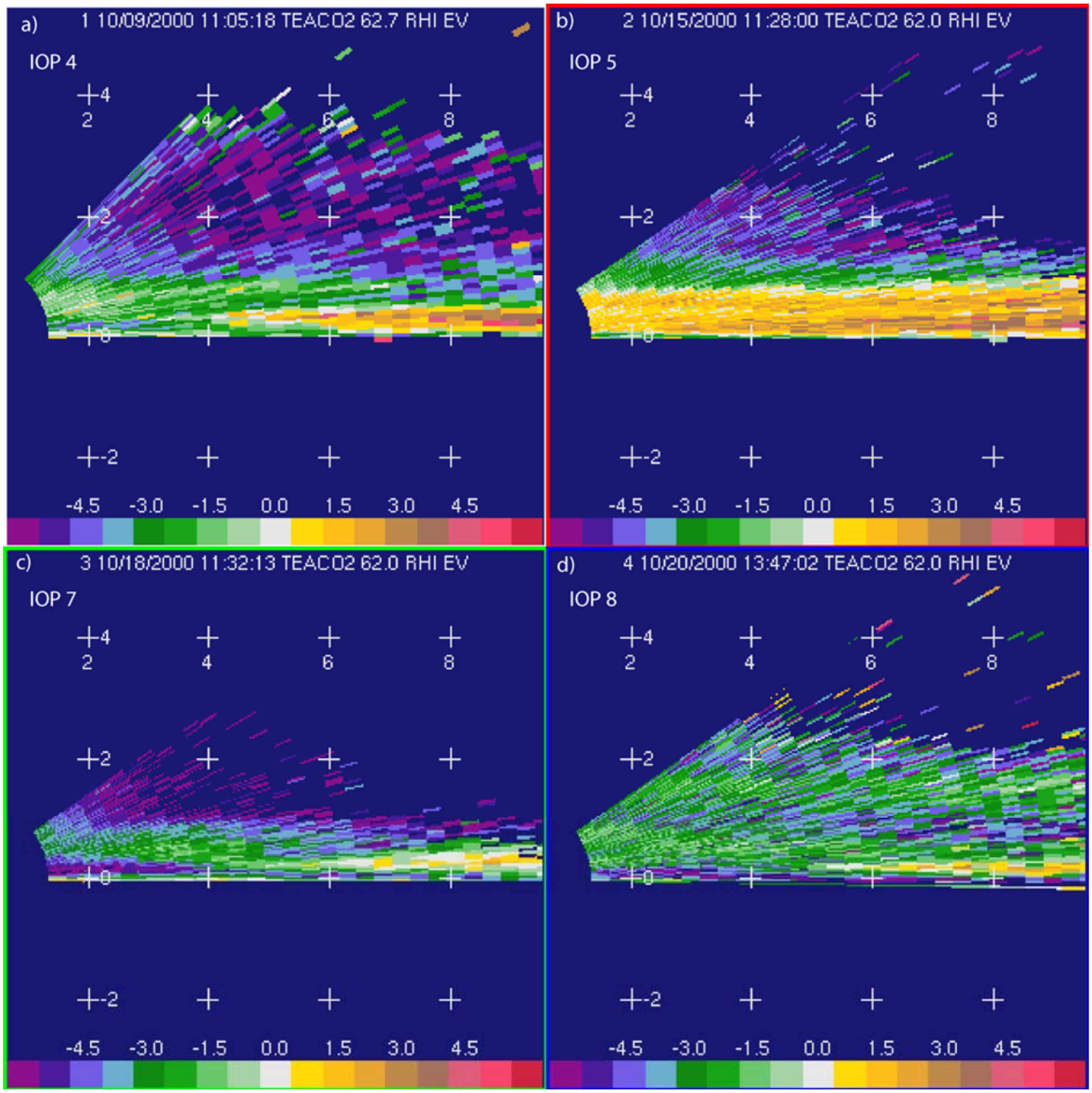

Figure 3: Doppler lidar range-height scans pointing toward Parleys Canyon (Figs 1 and 2). The color bar at the bottom of the plot indicates radial velocity in m s^{-1}. Positive velocities indicate flow toward the lidar, which is located in the lower left-hand corner. a) IOP 4, b) IOP 5, c) IOP 7, and d) IOP 8. The IOP 4, 7, and 8 scans show a shallow outflow (yellow/orange) emanating from Parleys Canyon into the basin. IOP 5 had a much deeper outflow.

3. RESULTS

Figure 4 is a time-height cross-section showing the evolution of the southerly LLJ for IOPs 4-8. The profiles of the horizontal wind that were used to construct these cross sections were derived from a window 7 to 9 km south of the lidar, pointing toward the opening of the Jordan Narrows (Fig. 1). The solid contours represent northerly-component flow along the plane of the lidar scan. The dashed lines represent southerly-component flow, the LLJ. In IOPs 4, 5, 7, and 8 the onset of the LLJ, signified by the zero-line (bold contour), was distinct, with a clear-cut reversal in the wind component. IOP 6 had a less distinct reversal. The LLJ during IOPs 4 and 7 tended to be at least 1 km deep with a continual strengthening of the winds throughout the night. During IOPs 6 and 8 the LLJ started out shallow and gained depth and speed throughout the night. The LLJ for IOP 5 was unique among the IOPs in that it

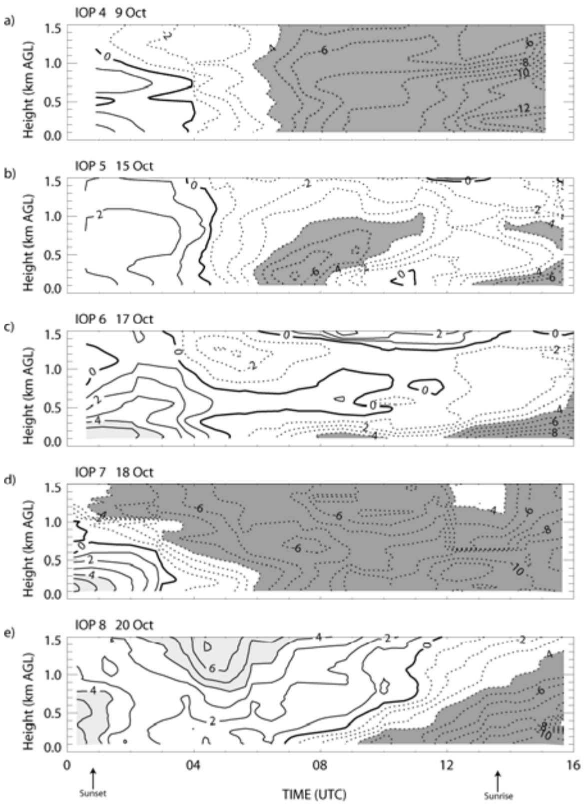

Figure 4: Time-height series of the horizontal component of the lidar-measured wind derived from range-height scans pointing toward the Jordan Narrows gap. Solid lines indicate northerly component flow. Dashed lines indicate southerly component flow. Magnitudes ≥ 4 m s^{-1} are shaded.

had a period of significant weakening, especially between 1000 and 1100 UTC.

3.1 *Overview of IOP 4*

We begin with an overview of IOP 4 to introduce the features of interest that occur in the all of the IOPs, and as a foundation for discussing the other IOPs. Figure 5 shows the lidar-measured winds for IOP 4. The top panel is the time-height series indicating the inflows (solid contours) and outflows (dashed contours) for PAR (62º azimuth relative to the lidar), the middle plot shows the inflows and outflows for BCC (94º azimuth), and the bottom panel contains the wind profiles derived from 10º elevation conical scans, centered at the lidar site. The shear blue box denotes the transition period between the time of the LLJ onset and when it reached a speed of 4 m s^{-1} (based on the low-level measurements shown in Fig. 4).

Before the LLJ reached a speed of 4 m s^{-1}, both PAR and BCC had weak winds flowing into the basin (Fig. 5). The double-ended arrow above the PAR plot, with the letters NE after it, indicates that during this time the ridge-top winds were from the northeast. It was expected that upper-level flow from the northeast would enhance the canyon outflows, but this does not appear to be the case at this time. Figure 2a shows the distinct outflows during this period.

After the LLJ reached a speed of 4 m s^{-1} (to the right of the blue box), the wind component for both canyons reversed to inflow, with PAR having a much stronger inflow. By 1000 UTC, a very shallow (~200 m deep) and weak outflow from PAR penetrated into the basin, lasting only 3 hr (Figs. 3a and 5). BCC, on the other hand, developed a much stronger and deeper outflow component after 1000 UTC. This is possibly due to the differences in orientation of the two canyons. Since PAR is slightly more northeast-southwest oriented than BCC, it may be easier for a southerly-component flow to extend into the canyon with time, preventing the outflow from extending into the basin.

Given the character of the PAR outflow, it is likely it was a thermally-driven outflow (colder, denser air leaving the canyon, in opposition to the basin-scale southerly flow). During the last 3 hr of the IOP 4 time series the ridge-top winds had become southwesterly (indicated by the double-ended arrow at the top of the plot). It was expected that southwesterly flow aloft, along with the LLJ, would inhibit canyon outflow penetration into the basin. This appeared to be the case for PAR, but did not seem to be the case for BCC. The analysis is hampered by the fact that air in the basin had become cleaner, limiting the range of the lidar measurements to the east of the lidar, at low elevation angles, to 10 km during this time, making it impossible to determine exactly what was happening at BCC.

3.2 *All IOPs*

During all IOPs, both canyons exhibited weak outflows before the LLJ onset, as seen during IOP4 (Figs. 2, 5-9). After LLJ onset, as seen in IOP 4, the PAR outflows were shut down or interrupted between the onset of the southerly flow and when the southerly flow reached a speed of 4 m s^{-1} (compare Fig. 4 with top panels of Figures 5-9). During IOPs 4 and 7, those with a strong and deep LLJ, PAR outflow either did not form again after the onset of the LLJ (IOP 7, Fig.

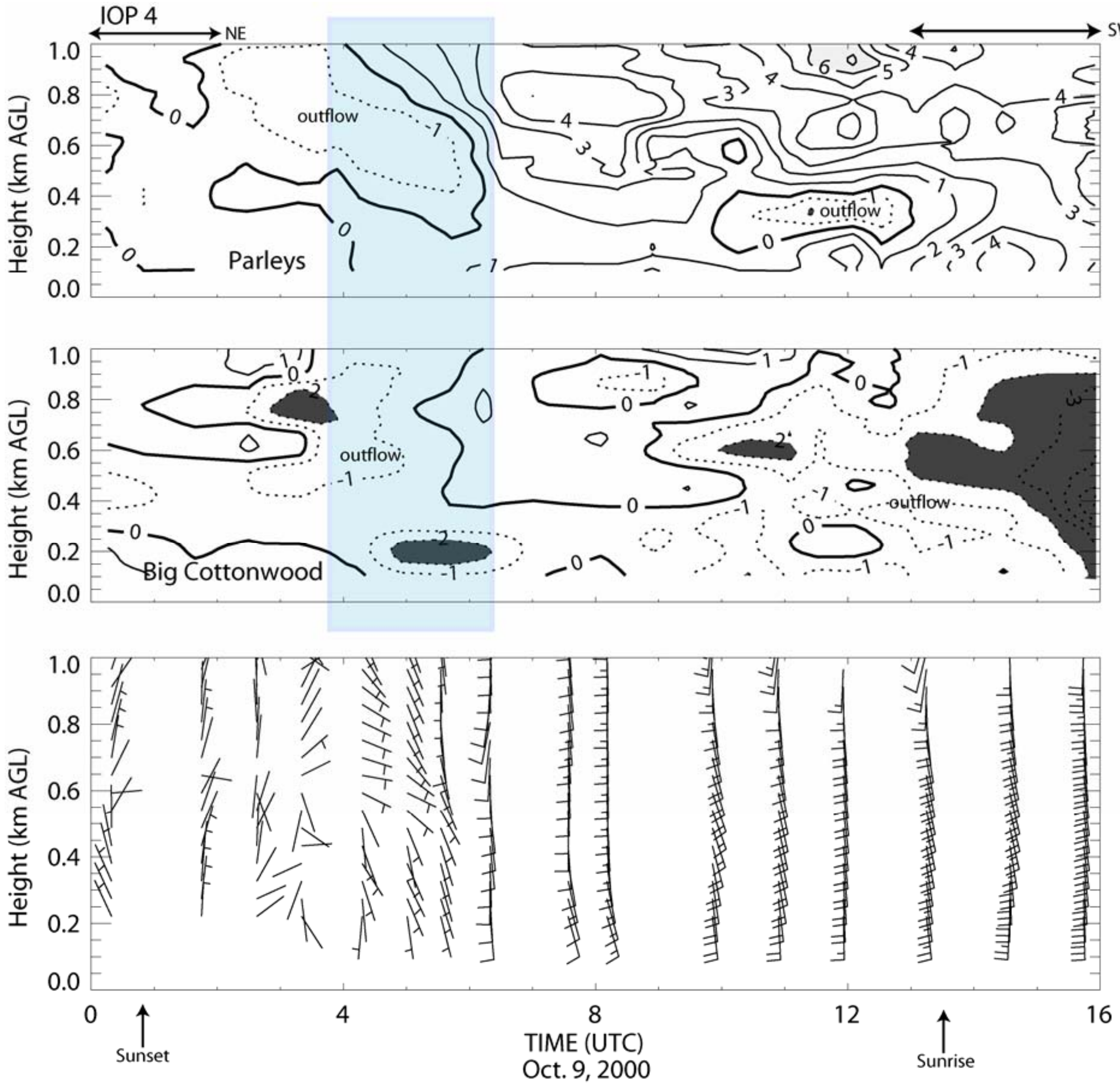

8),

Figure 5: Lidar-measured winds from IOP 4. The top panel indicates the horizontal component of the wind derived from range-height scans pointing toward Parleys Canyon. The middle panel is for Big Cottonwood Canyon. The bottom panel shows vertical profiles of the horizontal wind derived from conical lidar scans. Additional annotation includes a blue box which indicates the onset and early development of the southerly low-level jet. Double-ended arrows at the top indicate when the ridge-top winds were from the southwest or northeast (i.e., parallel to Parleys Canyon and nearly parallel with Big Cottonwood Canyon). Flow toward the basin ≥ 2 m s^{-1} is shaded.

or came back as a weak, elevated, shallow outflow that lasted only 3 hr (IOP 4, Fig. 5). There was no hint of this outflow in the wind profiles (Fig. 5, bottom panel), indicating that the outflow was too shallow to be detected by the 10º elevations scans. During IOPs 5, 6, and 8, the outflows did reappear in the basin later in the evening. IOP 5 had a deeper and longer-lived outflow component (Fig. 3b and 6). IOP 8 had a very thin layer of weak low-level outflow (Figs. 3d and 9). IOP 7 had a very weak short-lived outflow that barely registered in the time-height series (Figs. 3c and 8).

There were less obvious changes in the BCC flows associated with the onset or strengthening of the LLJ: either a weakening of the outflows or a reversal to inflow, seen in the middle panels of Figs. 5-9. After the outflow weakening or reversal, the BCC outflow returned during all IOPs, with IOPs 4, 5, and 8 having

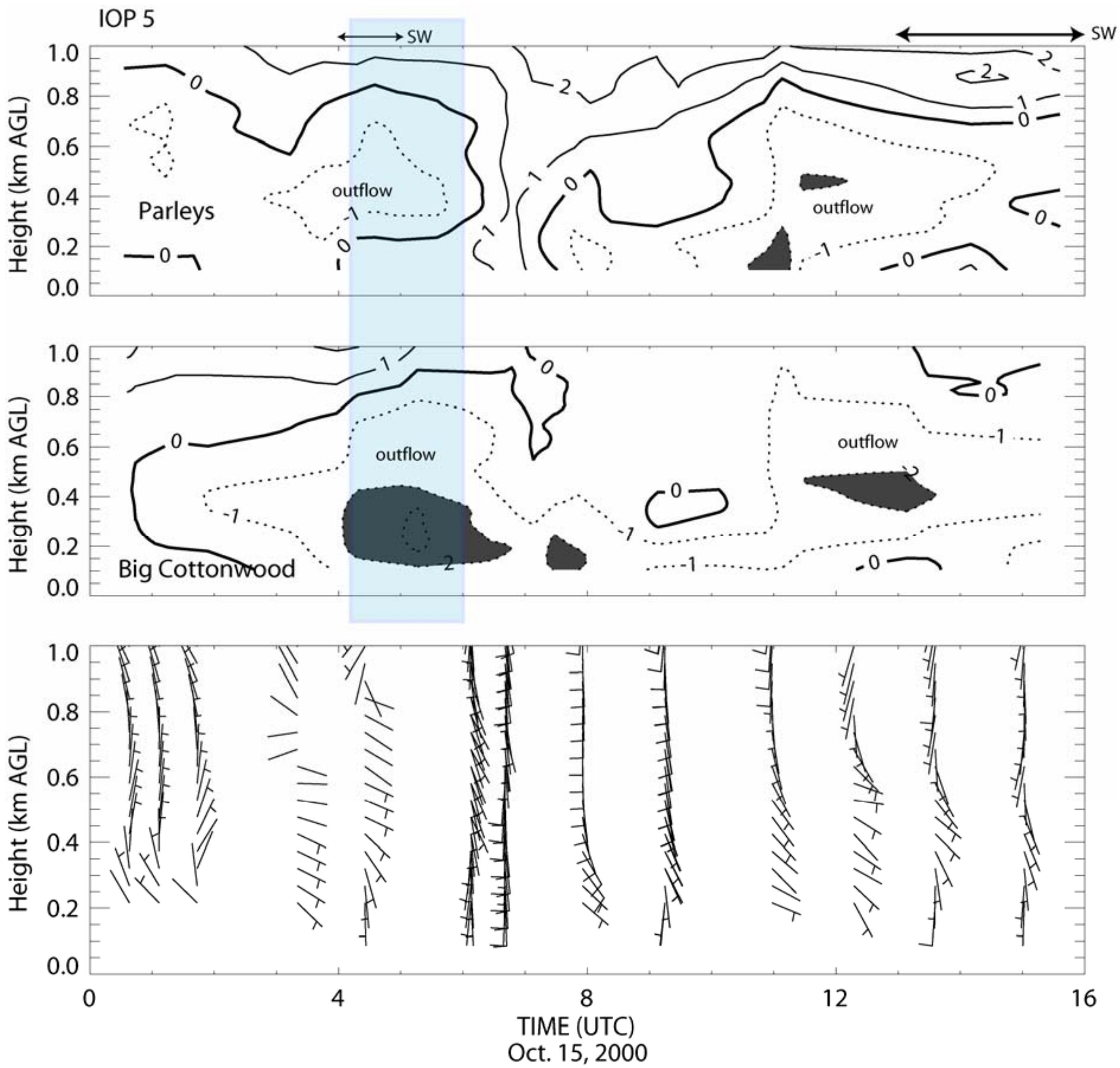

Figure 6: The same as Figure 5, except for IOP 5.

outflows ≥ 2 m s $^{-1}$ and IOP 6 having very weak winds in general.

The differences in the measured response of the canyon flows to the LLJ onset may in part be explained by the geometry of the canyons relative to the lidar. The Doppler lidar was able to scan parallel to PAR's axis, but that was not the case for BCC (Fig. 1). Thus, when the lidar beams were pointing toward the opening of BCC, they were not necessarily parallel to the outflow. Differences in canyon geography may also play a role in the differences in the responses.

3.3 *Ridge-top winds*

Next we look at ridge-top (R-T, ~1 to 1.2 km AGL) winds and how they influenced the canyon flows. IOP 7 was similar to IOP 4. The last three hours of both time series included southwesterly flow above R-T, yet the behavior of the flows associated with each canyon during the period of strong southwest R-T flow was quite different. During the last 3 hr of the time series, BCC had the strongest outflow of the IOP during IOP4 (Fig. 5) but very weak outflow was seen during IOP 7 (Fig. 8), which is in opposition to the R-T winds. Meanwhile, PAR had solid inflow during this period for both IOPs (Figs. 5 and 8). IOP 5 also had southwesterly flow above R-T during the last 3 hours of the time series, but it

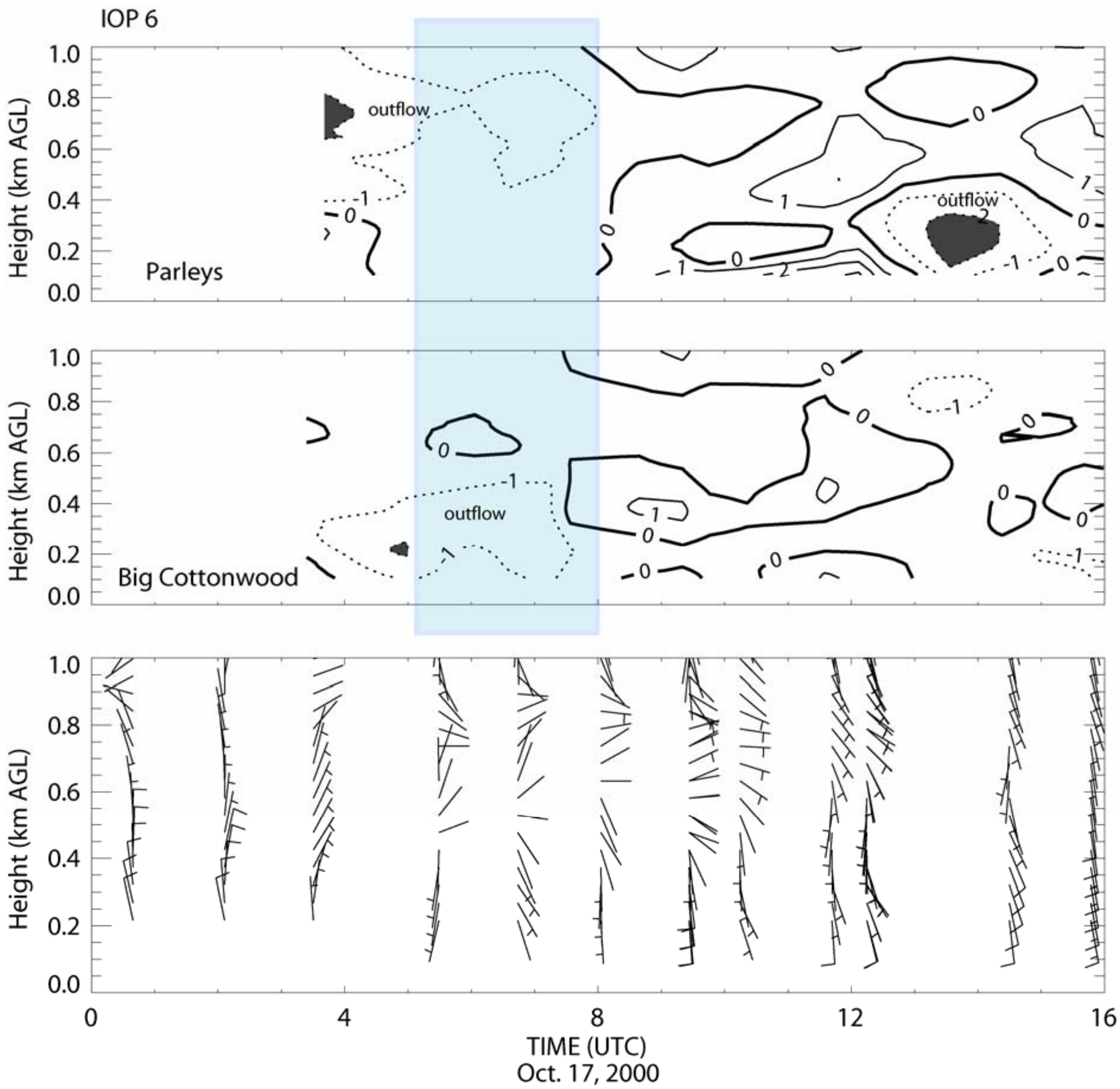

Figure 7: The same as Figure 5, except for IOP 6.

was weaker than during the other IOPs (5 m s^{-1} as opposed to 10-15 m^{-1}). Both canyons had weak outflows during this time and did not appear to be strongly influenced by the southwest flow aloft (Fig. 6).

IOP 8, with a noticeable slow veering of the winds above and below R-T throughout the evening, had enhanced outflow when the R-T winds were northeasterly. Because of the veering winds, PAR experienced an outflow of ≥ 2 m s^{-1} before BCC did. IOP6 had light and variable winds at R-T and weak LLJ flow. The two canyons responded differently to the conditions, with PAR having a relatively deep and well-defined canyon outflow while the BCC winds remained ± 1 m s^{-1} throughout the evening.

4. CONCLUSIONS

Outflows from the canyons along the east wall of the basin were found to be strongly influenced by the onset and development of a southerly LLJ, and also influenced, but to a lesser degree, by R-T winds. Certain threshold values became apparent during the analysis of the wind component aligned with the openings of two canyons that drain into the Salt Lake City basin when compared to the life-cycle of a low-level jet and ridge-top winds: 1) when the southerly basin-scale flow reached a speed of 4 m s^{-1}, the

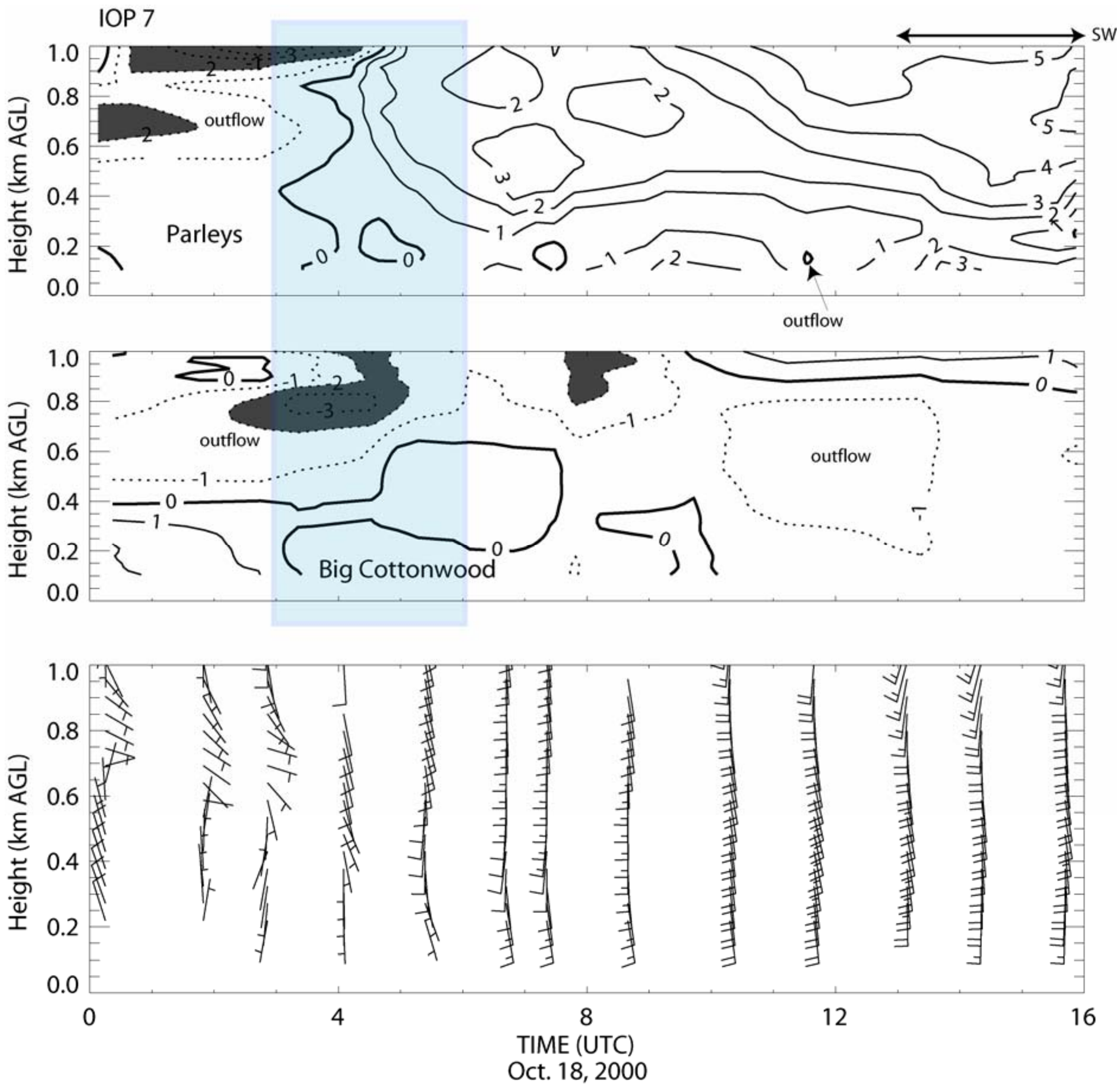

Figure 8: The same as Figure 5, except for IOP 7.

penetration of the PAR and BCC canyon outflows into the basin was shut down either temporarily or for the rest of the night, and 2) when southwesterly ridge-top winds were ≥ 10 m s^{-1} , they had a strong impact on PAR by enhancing winds in the inflow direction and hampering outflow penetration into the basin, but had a weaker effect on the BCC outflow. The LLJ and ridge-top winds are, in turn, controlled by synoptic-scale factors such as surface pressure gradient (Banta et al. 2004) and upper-level waves and ridges.

Another factor that requires investigation is the geometry of the canyons, such as the width of the canyons from side wall to side wall and the slopes of the canyon side walls, both of which would affect the formation and strength of thermally-driven drainage flows, as well as their penetration into the Salt Lake City basin.

5. ACKNOWLEDGMENTS

This work was supported by the U.S. Department of Energy, under the auspices of the Environmental Meteorology Program of the Office of Biological and Environmental Research, through Interagency Agreements DE-AI03-99ER62842 and DE-AI02-04ER63860. We also wish to express our gratitude to the lidar crew: Raul Alvarez, Alan Brewer, Sherlyn Cooley, Janet Intrieri, Brandi McCarty, Richard Marchbanks, and Scott Sandberg, and Jim Howell.

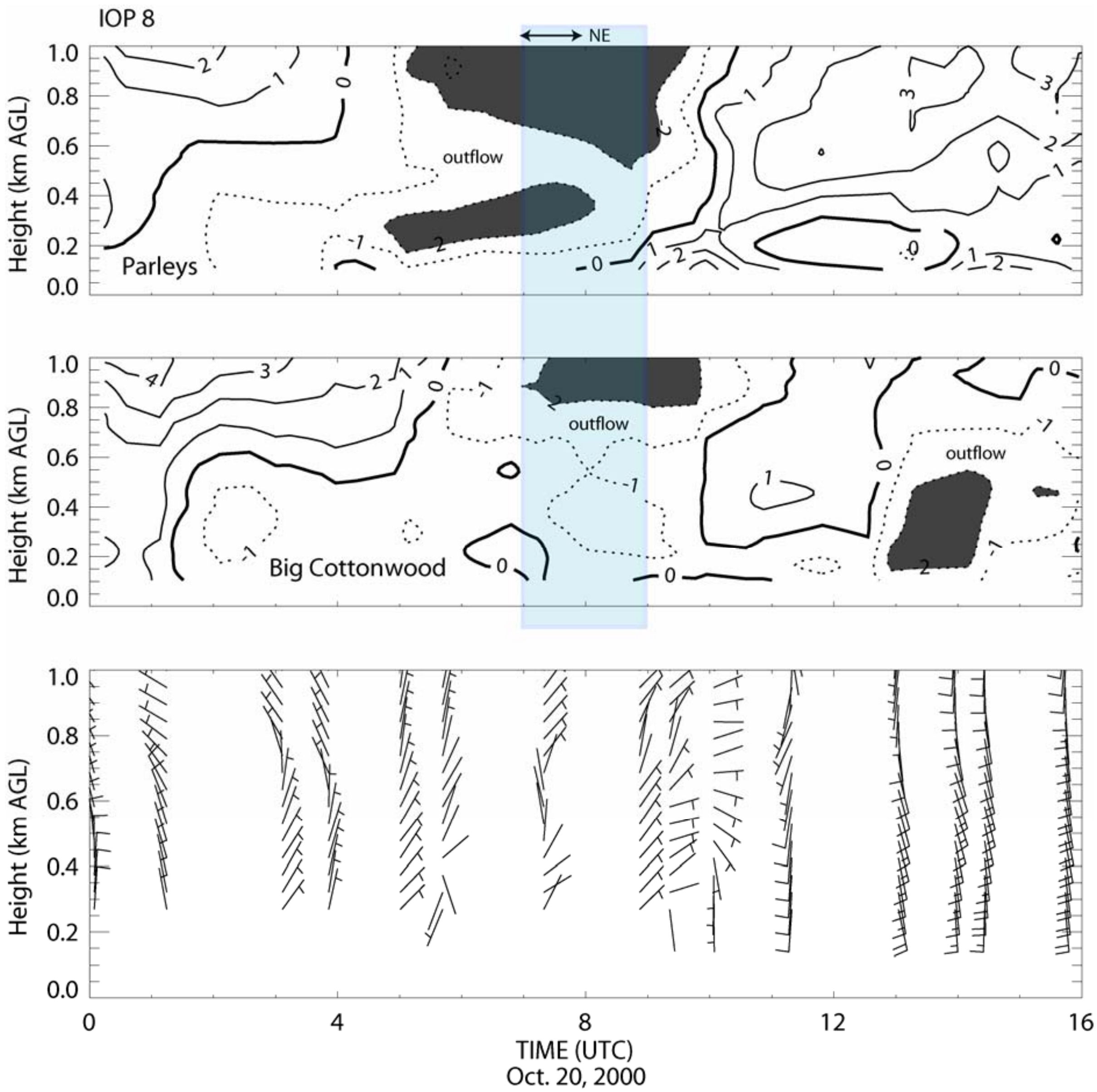

Figure 9: The same as Figure 5, except for IOP 8.

6. REFERENCES

Banta, R. M., L. D. Olivier, and D. H. Levinson, 1993: Evolution of the Monterey Bay sea-breeze layer as observed by pulsed Doppler lidar. *J. Atmos. Sci.*, **50**, 3959-3982.

Banta, R.M., L.S. Darby, J.D. Fast, J. O. Pinto, C.D. Whiteman, W.J. Shaw, and B.D. Orr, 2004: Nocturnal low-level jet in a mountain basin complex I: Evolution and implications to other flow features. *J. Appl. Meteor.,* **43**, 1348-1365.

Browning, K.A., and R. Wexler, 1968: The determination of kinematic properties of a wind field using a Doppler radar. *J. Appl. Meteor.*, **7**, 105-113.

Darby, L.S., K.J. Allwine, and R.M. Banta, 2006: Nocturnal low-level jet in a mountain basin complex. Part II. Transport and diffusion of tracer under stable conditions. *J. Appl. Meteor.,* **45**, 740-753.

Doran, J.C., J.D. Fast, and J. Horel 2002: The VTMX 2000 campaign. *Bull. Amer. Meteor. Soc.*, **83**, 537-551.

Fast, J.D., and L.S. Darby, 2004: An evaluation of mesoscale model predictions of down-valley and canyon flows and their consequences using Doppler lidar measurements during VTMX 2000. *J. Appl. Meteor.,* **43**, 420-436.